View metadata, citation and similar papers at core.ac.uk

brought to you by CORE

provided by UNT Digital Library

SANDIA REPORT
SAND2007-1267
Unlimited Release
Printed March 2007

Joint Voltages Resulting from Lightning Currents

Larry K. Warne, William A. Johnson, Kenneth C. Chen, and Kimball O. Merewether

Prepared by
Sandia National Laboratories
Albuquerque, New Mexico 87185 and Livermore, California 94550

Sandia is a multiprogram laboratory operated by Sandia Corporation,
a Lockheed Martin Company, for the United States Department of Energy's
National Nuclear Security Administration under Contract DE-AC04-94AL85000.

Approved for public release; further dissemination unlimited.

Issued by Sandia National Laboratories, operated for the United States Department of Energy by Sandia Corporation.

NOTICE: This report was prepared as an account of work sponsored by an agency of the United States Government. Neither the United States Government, nor any agency thereof, nor any of their employees, nor any of their contractors, subcontractors, or their employees, make any warranty, express or implied, or assume any legal liability or responsibility for the accuracy, completeness, or usefulness of any information, apparatus, product, or process disclosed, or represent that its use would not infringe privately owned rights. Reference herein to any specific commercial product, process, or service by trade name, trademark, manufacturer, or otherwise, does not necessarily constitute or imply its endorsement, recommendation, or favoring by the United States Government, any agency thereof, or any of their contractors or subcontractors. The views and opinions expressed herein do not necessarily state or reflect those of the United States Government, any agency thereof, or any of their contractors.

Printed in the United States of America. This report has been reproduced directly from the best available copy.

Available to DOE and DOE contractors from
U.S. Department of Energy
Office of Scientific and Technical Information
P.O. Box 62
Oak Ridge, TN 37831

Telephone: (865) 576-8401
Facsimile: (865) 576-5728
E-Mail: reports@adonis.osti.gov
Online ordering: http://www.osti.gov/bridge

Available to the public from
U.S. Department of Commerce
National Technical Information Service
5285 Port Royal Rd.
Springfield, VA 22161

Telephone: (800) 553-6847
Facsimile: (703) 605-6900
E-Mail: orders@ntis.fedworld.gov
Online order: http://www.ntis.gov/help/ordermethods.asp?loc=7-4-0#online

SAND2007-1267
Unlimited Release
Printed March 2007

Joint Voltages Resulting from Lightning Currents

Larry K. Warne and William A. Johnson
Electromagnetics and Plasma Physics Analysis Dept.

Kenneth C. Chen
Nuclear Safety Assessment Dept.

Kimball O. Merewether
Weapon Surety Engineering Dept.

Sandia National Laboratories
P. O. Box 5800
Albuquerque, NM 87185-1152

Abstract

Simple formulas are given for the interior voltages appearing across bolted joints from exterior lightning currents. External slot and bolt inductances as well as internal slot and bolt diffusion effects are included. Both linear and ferromagnetic wall materials are considered. A useful simplification of the slot current distribution into linear stripline and cylindrical parts (near the bolts) allows the nonlinear voltages to be estimated in closed form.

Intentionally Left Blank

Contents

Figures

Joint Voltages Resulting from Lightning Currents

Larry K. Warne and William A. Johnson
Electromagnetics and Plasma Physics Analysis Dept.

Kenneth C. Chen
Nuclear Safety Assessment Dept.

Kimball O. Merewether

Weapon Surety Engineering Dept.

Sandia National Laboratories
P. O. Box 5800
Albuquerque, NM 87185

1 INTRODUCTION

Bolted joints allow interior access to conducting enclosures, such as, weapon systems. Figure 1 shows a simple example of such a cylindrical bolted joint. Tortuous depth path configurations as shown in Figure 2, created by standard bolted joints with flush interior and exterior surfaces, have similar electrical properties, provided the depth d represents the total distance along the slot depth between the exterior and interior surfaces. Other types of overlap, as shown in Figure 3, are treated similarly.

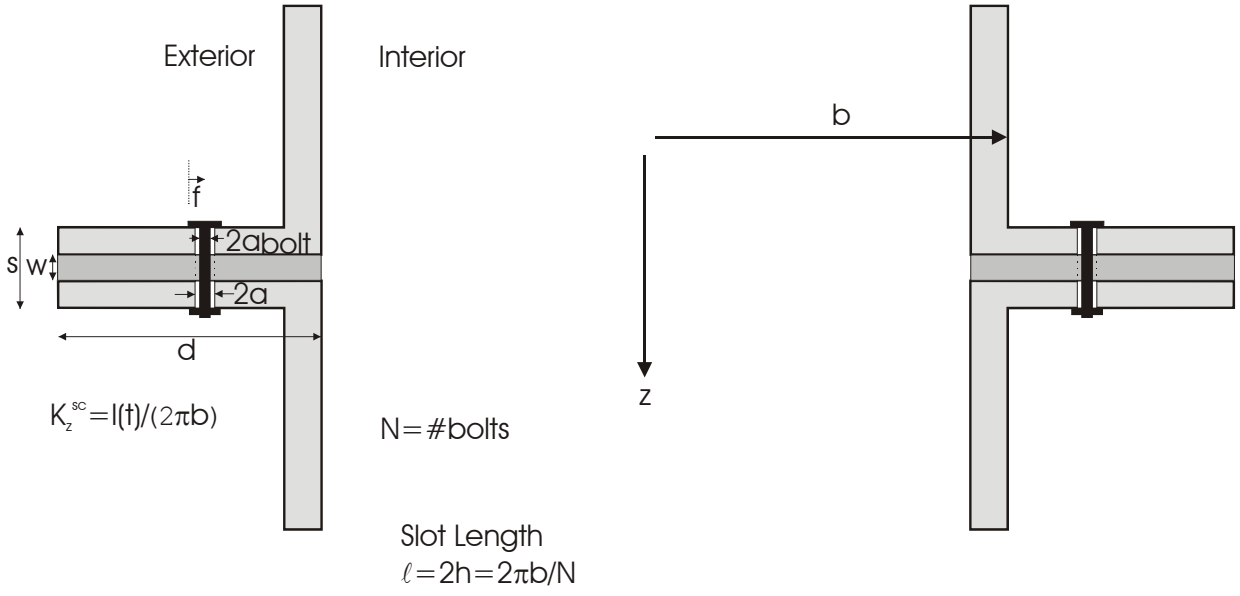

Figure 1. Example of bolted cylindrical joint.geometry.

If lightning current flows down the exterior surface across the joint, voltages are created and appear on the interior of the system. These voltages are of concern for several reasons: if multipoint circuit grounds exist on opposite sides of the joint, the interior joint voltage drives currents directly on these circuits; even if multipoint grounds are not used, it may be possible for this voltage to be large enough that arc paths could be established to conductors passing near the interior joint surfaces. It is thus useful to construct simple

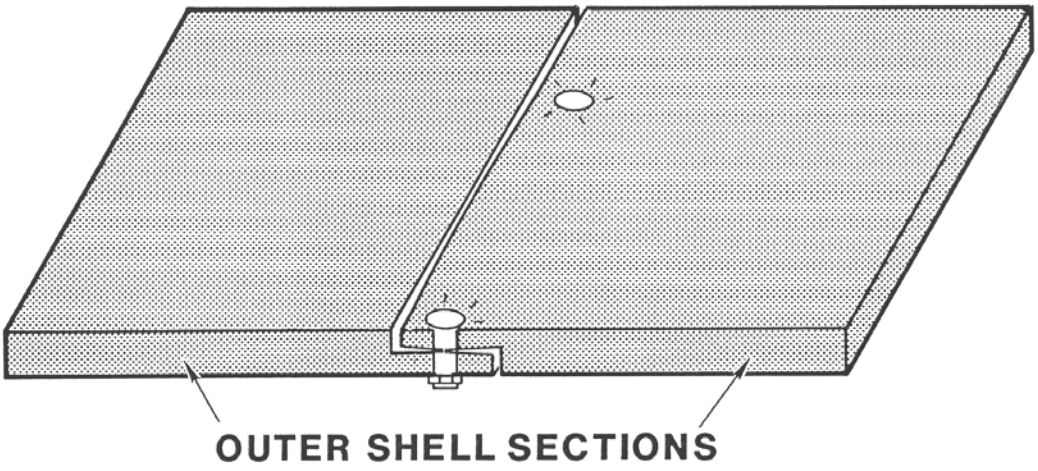

Figure 2. Bolted joint with tortuous depth path between flush exterior and interior surfaces.

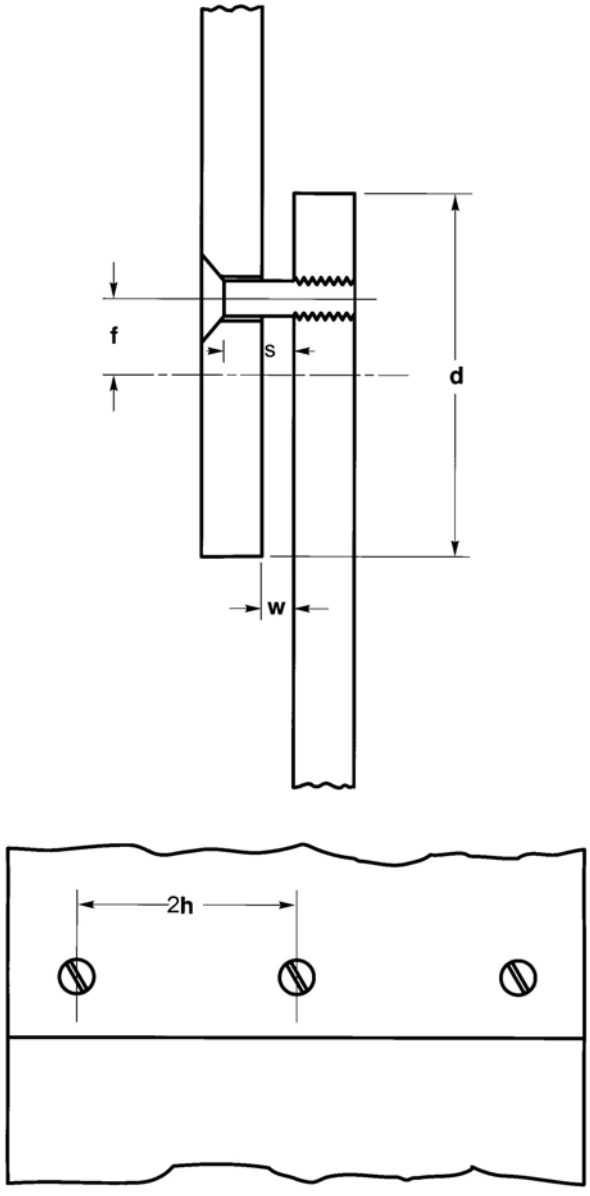

Figure 3. Overlap screw joint.

models for the interior joint voltages that can be quickly used to assess the importance of these concerns. The models discussed in this report have been used to interpret experimental joint voltage measurements [1].

The next section considers the external inductance of the bolted joint slots. The transfer inductance is found as a modal series for general bolt positions; for a centered bolt a simple and accurate fit function is given. This fit function can be viewed as arising from a useful simplification of current distribution in the slot, consisting of a linear stripline distribution in addition to a cylindrical distribution converging on the bolt with an effective outer radius. The following sections consider the internal wall impedance for both linear and nonlinear (ferromagnetic) wall materials; the approximate two part current distribution allows the nonlinear voltage to be estimated in closed form. Coaxial bolt loads are next added to complete the bolted joint models. The peak interior voltages are approximated in closed form by linearizing the rising portion of the lightning current waveform. The final two sections investigate the contribution near the bolt hole when the penetration depth is large compared to the hole radius; the nonlinear (ferromagnetic) wall voltage is also determined numerically and compared to the result using the two part approximate current distribution.

2 EXTERNAL INDUCTANCE OF BOLTED JOINT SLOT

Unlike an array of rectangular waveguides, the bolted joint slots are separated by single bolts in the depth dimension, and thus static decay of the fields (at low frequencies) will not necessarily be present. The simplest configuration thus results when the bolted joint slots are driven symmetrically [2]. This configuration also results in the worst case interior voltage (for a given uniform current density per slot), and is thus the natural case to examine for bounding the response even under asymmetric drive situations. We assume if the joint is cylindrical that the radius of curvature b is large compared to the bolt spacing ℓ (or $N_{slot} >> 1$). Thus we can consider only the planar model shown in Figure 4.

Between bolts (with symmetric drive conditions) perfect magnetic conductor (PMC) symmetry conditions hold; thus we may consider only a single bolt with boundary conditions on the magnetic field intensity

$$H_y(\pm h, y) = 0 \tag{1}$$

where $\ell = 2h$ is the slot length and the bolt spacing. A uniform current density K_z^{sc}, found from

$$2hK_z^{sc} = I_{tot}/N_{slot} = I \tag{2}$$

where I_{tot} is the total lightning current, N_{slot} is the number of slots, and I is the current through a single bolt, excites the exterior slot face as shown in Figure 4. Assuming that the slot width w is small compared to the slot depth d, the exterior inductive loading of the slot can be approximately ignored [3]. The interior and exterior slot faces are thus also approximate PMCs, except that the exterior face has the forced short circuit current density

$$H_x(x, -d/2) \approx H_x^{sc} = K_z^{sc} \tag{3}$$

$$H_x(x, d/2) \approx 0 \tag{4}$$

The solution is constructed by using the magnetic vector potential $\underline{A}$ where the magnetic induction is

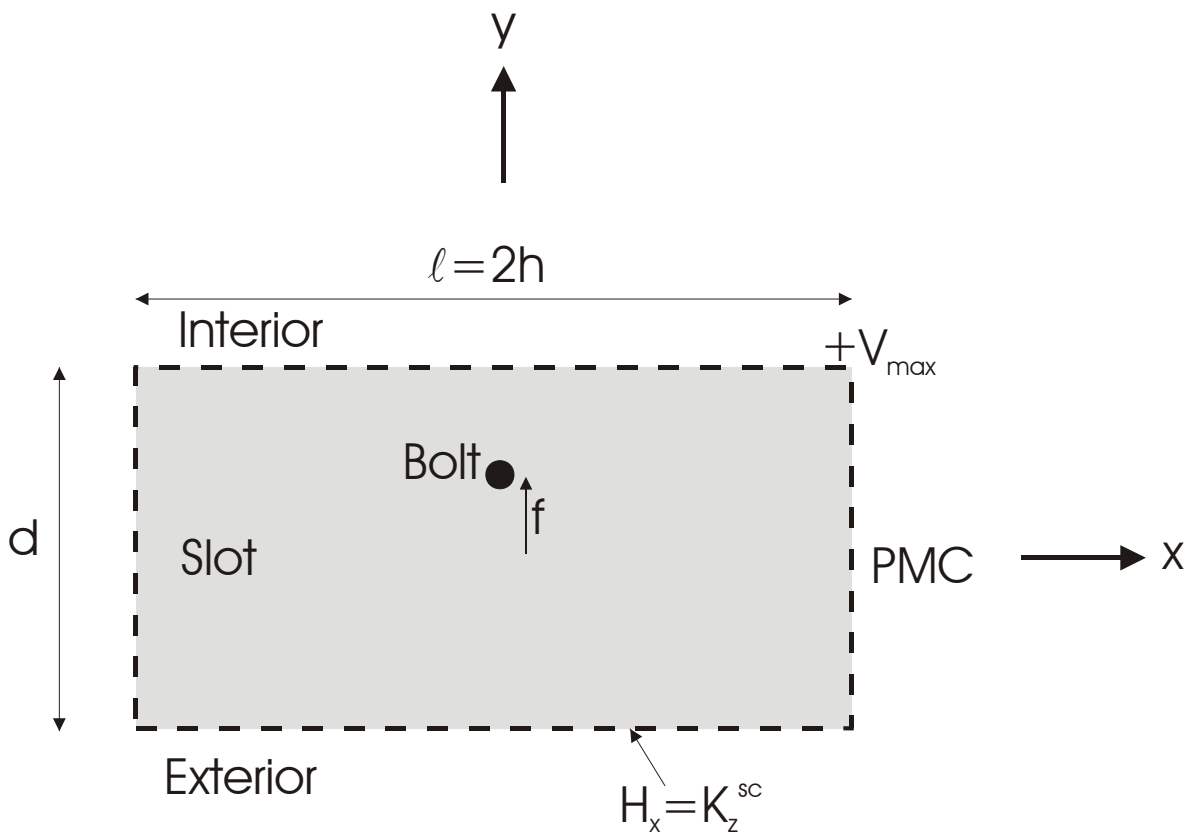

Figure 4. Approximate planar equivalent of symmetric single bolt joint.

$\underline{B} = \mu_0 \underline{H} = \nabla \times \underline{A}$ and $\mu_0 = 4\pi \times 10^{-7}$ H/m is the free space magnetic permeability. Choosing the Coulomb gauge $\nabla \cdot \underline{A} = 0$ and using Ampere's law $\nabla \times \underline{H} = \underline{J}$ gives $\nabla^2 \underline{A} = -\mu_0 \underline{J}$, where the electric current density is $\underline{J}$. Here we represent the bolt current by the component J_z. The bolt hole radius a is assumed to be much less than the distance $d/2 - |f|$ so that we can treat it as a filament current. The magnetic vector potential of the problem has only a z component satisfying

$$\nabla_t^2 A_z = -\mu_0 J_z = -\mu_0 I \delta(x)\delta(y - f) \tag{5}$$

where $\nabla_t^2 = \frac{\partial^2}{\partial x^2} + \frac{\partial^2}{\partial y^2}$ is the transverse Laplacian operator and $\delta(x)$ is the Dirac delta function. The transverse magnetic field $\underline{H}_t$ is found from

$$\mu_0 \underline{e}_z \times \underline{H}_t = \nabla_t A_z \tag{6}$$

where $\underline{e}_z$ is the axial unit vector.

It is convenient to first construct the solution of the slot when $d \to \infty$ denoted as A_z^∞. This solution which satisfies the boundary conditions (1) can be written as

$$A_z^\infty = -\frac{\mu_0 I}{2\ell} |y - f| + \frac{\mu_0 I}{\pi} \sum_{n,\ \text{even}} \frac{1}{n} (-1)^{n/2} \cos \frac{n\pi}{\ell} (x + h) e^{-|y-f| n\pi/\ell} \tag{7}$$

where the symmetry in x eliminates the odd terms in the series. Alternatively conformal mapping, with complex variable $z = x + iy$, can be used to determine the solution as the real part of a complex potential $A_z^\infty = \text{Re}(W)$. We can take the complex potential to be $W = -\frac{\mu_0 I}{2\pi}[\ln(z_1 - z_1') + \ln(z_1 - z_1'^*) - \ln(z_1) + C]$ where the conformal transformation that maps the strip $|\text{Re}(z)| < h$ into the upper half plane $\text{Im}(z_1) > 0$ is $z_1 = ie^{-i\pi z/\ell}$ (the source point is $z_1' = ie^{\pi f/\ell}$). The constant C can be determined to match the values of the conformal mapping solution to the modal solution (7) as $|y| \to \infty$ (and thus make the two solutions identical)

$$A_z^\infty = -\frac{\mu_0 I}{2\pi} \ln \left| e^{-i\pi z/h} - e^{\pi f/h} \right| + \frac{\mu_0 I}{2\ell} (y + f) \tag{8}$$

The total vector potential, including the boundary conditions (3) and (4), can be written as

$$A_z = A_z^\infty + A_z^B \tag{9}$$

where the boundary part is solved using the representation (7)

$$A_z^B = B_0 + C_0 y + \sum_{n,\ \text{even}} \left[B_n \cosh\left(\frac{n\pi}{\ell} y\right) + C_n \sinh\left(\frac{n\pi}{\ell} y\right) \right] \cos \frac{n\pi}{\ell} (x + h) \tag{10}$$

The arbitrary constant B_0 can be dropped. Enforcing the boundary conditions (3) and (4), gives

$$C_0 = \frac{1}{2} \mu_0 K_z^{sc} = \frac{\mu_0 I}{2\ell} \tag{11}$$

$$C_n = \frac{\mu_0 I}{n\pi} (-1)^{n/2} e^{-n\pi d/(2\ell)} \frac{\sinh(n\pi f/\ell)}{\cosh(n\pi d/(2\ell))} \tag{12}$$

$$B_n = \frac{\mu_0 I}{n\pi} (-1)^{n/2} e^{-n\pi d/(2\ell)} \frac{\cosh(n\pi f/\ell)}{\sinh(n\pi d/(2\ell))} \tag{13}$$

The magnetic flux passing through the surface S can be found from

$$\Phi = \int_S \underline{B} \cdot \underline{n}\, dS = \oint_C \underline{A} \cdot \underline{d\ell} \tag{14}$$

where $\underline{n}$ is the unit normal to S and the contour C is the boundary of S. The maximum interior voltage occurs at the points between bolts $x = h$, $y = d/2$ as shown in Figure 4. The magnetic flux (14) between the bolt hole and this point is therefore

$$\Phi = w\left[A_z(0, f+a) - A_z(h, d/2)\right] = L_{\max} I \tag{15}$$

where $L_{\max}$ is an inductance. The value of this inductance, using (8), (10), (11), (12), and (13), is

$$\frac{2\pi}{\mu_0 w} L_{\max} = -\ln\left(1 - e^{-\pi a/h}\right) + \ln\left\{1 + e^{\pi(2f-d)/\ell}\right\}$$

$$-\sum_{n=1}^{\infty} \frac{1}{n} e^{-n\pi d/\ell} \left[\frac{\cosh(n\pi f/h)}{\sinh(n\pi d/\ell)} \left\{(-1)^n \cosh\left(\frac{n\pi d}{\ell}\right) - \cosh\left(\frac{n\pi}{h}(f+a)\right)\right\}\right.$$

$$\left. + \frac{\sinh(n\pi f/h)}{\cosh(n\pi d/\ell)} \left\{(-1)^n \sinh\left(\frac{n\pi d}{\ell}\right) - \sinh\left(\frac{n\pi}{h}(f+a)\right)\right\}\right] \tag{16}$$

For small a we can approximate this result by

$$\frac{2\pi}{\mu_0 w} L_{\max} \approx \ln\left(\frac{h}{\pi a}\right) + O(a) + \ln\left\{1 + e^{\pi(2f-d)/\ell}\right\} - \sum_{n=1}^{\infty} \frac{1}{n} e^{-n\pi d/\ell}$$

$$\left[\frac{\cosh(n\pi f/h)}{\sinh(n\pi d/\ell)} \left\{(-1)^n \cosh\left(n\pi d/\ell\right) - \cosh\left(n\pi f/h\right)\right\}\right.$$

$$\left. + \frac{\sinh(n\pi f/h)}{\cosh(n\pi d/\ell)} \left\{(-1)^n \sinh\left(n\pi d/\ell\right) - \sinh\left(n\pi f/h\right)\right\}\right] \tag{17}$$

If we set $f = 0$ in (16) we find

$$\frac{2\pi}{\mu_0 w} L_{\max} = -\ln\left(1 - e^{-\pi a/h}\right) + \ln\left(1 + e^{-\pi d/\ell}\right) - \sum_{n=1}^{\infty} \frac{1}{n} e^{-n\pi d/\ell}$$

$$\frac{1}{\sinh(n\pi d/\ell)} \left\{(-1)^n \cosh\left(n\pi d/\ell\right) - \cosh\left(n\pi a/h\right)\right\} \tag{18}$$

If we approximate this expression for small a, but keep the first term intact we obtain

$$\frac{2\pi}{\mu_0 w} L_{\max} = -\ln\left(1 - e^{-\pi a/h}\right) + O(a^2) + \ln\left(1 + e^{-\pi d/\ell}\right)$$

$$-\sum_{n=1}^{\infty} \frac{1}{n} e^{-n\pi d/\ell} \frac{1}{\sinh(n\pi d/\ell)} \left\{(-1)^n \cosh\left(n\pi d/\ell\right) - 1\right\} \tag{19}$$

The form of the first term coincides with the form often used in the wire grid problem [2]; it yields useful values even when a is pushed to larger values than can be rigorously justified (the value of the first term remains positive for example). (In the one dimensional array or wire grid problem $d \to \infty$, the approximate form of this logarithm $\ln\left(\frac{h}{\pi a}\right)$ gives a more accurate transfer inductance, for small values of a, than $-\ln\left(1-e^{-\pi a/h}\right)$; this can be demonstrated by including the line dipoles of the wires [4].)

Asymptotic limits of (17) are [3]

$$L_{\max} = \frac{\mu_0 w}{2\pi} \ln\left(\frac{h}{\pi a}\right) \ , \ \frac{d}{\ell} \to \infty$$

$$L_{\max} \sim \frac{1}{4} h \mu_0 \frac{w}{d} + \frac{\mu_0 w}{2\pi} \ln\left[\frac{d/(2\pi a)}{\cos(\pi f/d)}\right] \ , \ \frac{d}{\ell} \to 0 \tag{20}$$

For $f = 0$ a function which incorporates these limits is

$$L_{\max} \approx \frac{1}{4} h \mu_0 \frac{w}{d} + \frac{\mu_0 w}{2\pi} \ln\left[\left(\frac{hd/2}{h+d/2}\right)/(\pi a)\right] \tag{21}$$

A comparison of the function (21) and (17) (with $f = 0$), normalized by $\mu_0 w$, and both having the function of $\frac{1}{2\pi}\ln\left(\frac{h}{\pi a}\right)$ subtracted out, is given in Figure 5. Figure 6 shows the same results without removal of $\frac{1}{2\pi}\ln\left(\frac{\ell}{2\pi a}\right)$ for several values of ℓ/a.

Thus a very good approximation to (19) is

$$\frac{2\pi}{\mu_0 w} L_{\max} \approx \frac{\pi h}{2d} + \ln\left(\frac{d/2}{h+d/2}\right) - \ln\left(1-e^{-\pi a/h}\right) \tag{22}$$

The external contribution to the slot voltage V_{ext} is thus

$$V_{ext} = L_{\max} 2h \frac{\partial}{\partial t} K_z^{sc} = L_{\max} \frac{\partial}{\partial t} I \tag{23}$$

The simple linear approximation to the early time current

$$I(t) \approx (I_0/\tau_r)\, t \tag{24}$$

where τ_r is the rise time of the lightning current, gives

$$V_{ext} = L_{\max} I_0/\tau_r \tag{25}$$

3 LINEAR WALL VOLTAGE

The canonical model for the wall voltage contribution is taken as a planar half space diffusion problem. A conducting half space extends over $0 < z < \infty$ and has electrical conductivity σ and magnetic permeability μ. Maxwell's equations in the conductive half space $\nabla \times \underline{E} = -\frac{\partial}{\partial t}\underline{B}$ and $\nabla \times \underline{H} = \sigma \underline{E}$ and the constitutive relation $\underline{B} = \mu \underline{H}$ yield the diffusion equation

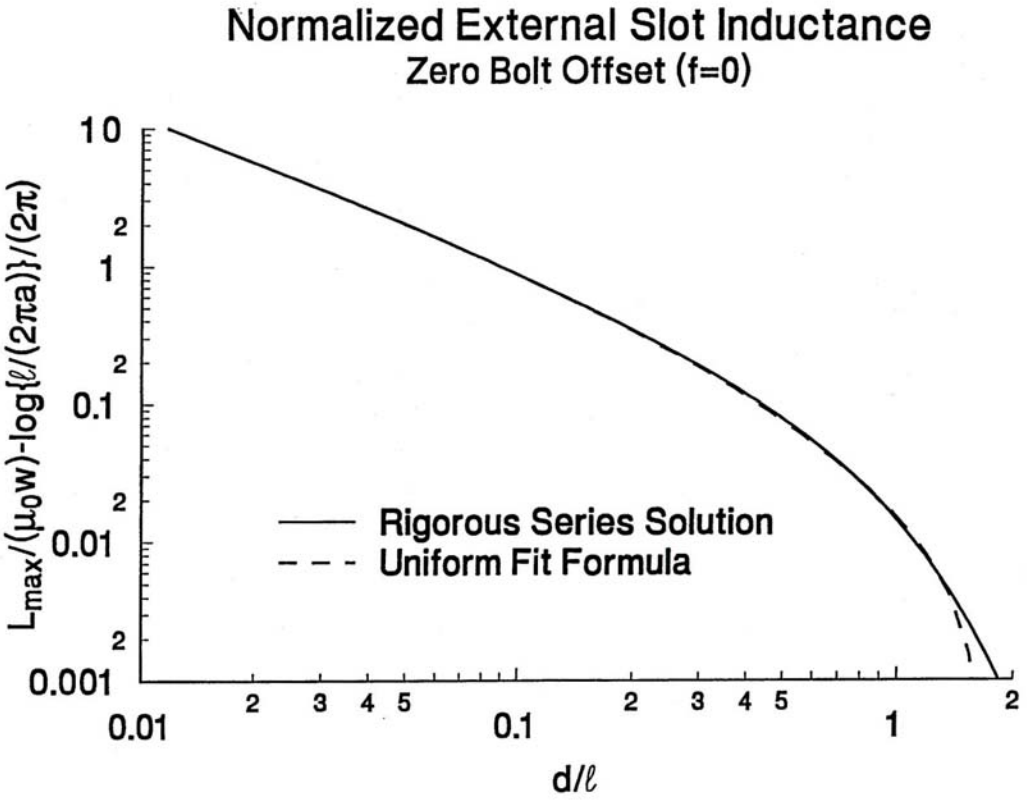

Figure 5. Comparison of simple fit formula with rigorous modal solution for external inductance in the centered bolt case with large depth asymptote removed.

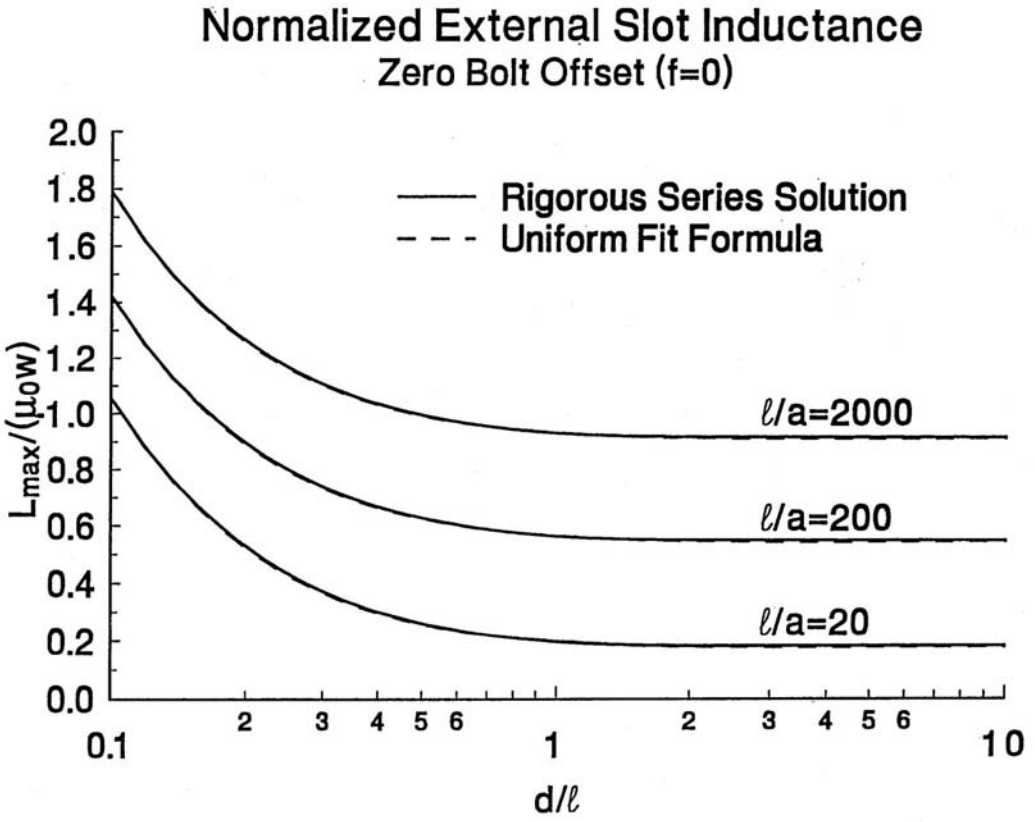

Figure 6. Comparison of simple fit formula with rigorous modal solution for external inductance in the centered bolt case.

$$\frac{\partial^2}{\partial z^2} H_y = \mu\sigma \frac{\partial}{\partial t} H_y \tag{26}$$

Given a surface magnetic field

$$H_0(t) = H_y(0,t) \tag{27}$$

the Laplace transform solution for the surface electric field $\sigma E_x = -\frac{\partial}{\partial z} H_y$ is thus

$$E_0(t) = E_x(0,t) = \frac{1}{2\pi i} \int_{r-i\infty}^{r+i\infty} H_0(s) \sqrt{s\mu/\sigma} e^{st} ds \tag{28}$$

where the Laplace transform of the surface magnetic field is

$$H_0(s) = \int_0^\infty e^{-st} H_0(t) dt \tag{29}$$

It is interesting that the properties of the Riemann Liouville fractional derivative [5] allow us to write the surface electric field as a function of the surface magnetic field

$$E_0\left(H_0\left(t\right)\right) = \sqrt{\mu/\sigma} \frac{d^{1/2}}{dt^{1/2}} H_0(t) \tag{30}$$

provided $H_0(t) = o(t^{-1/2})$ as $t \to 0$. When $H_0\left(t\right)$ is proportional to t^r we use the result $\frac{d^\beta}{dt^\beta} t^r = \frac{\Gamma(r+1)}{\Gamma(r+1-\beta)} t^{r-\beta}$, where $\Gamma\left(x\right)$ is the gamma function [5].

An alternative similarity solution (useful for power law $O(t^r)$ surface field behavior) can be obtained by substituting $H_y = t^r F\left(u\right), u = z\sqrt{\mu\sigma/(4t)}$ into (26); the function $F(u)$ is required to satisfy the ordinary differential equation

$$\frac{d^2F}{du^2} + 2u\frac{dF}{du} - 4rF = 0 \tag{31}$$

If $r = n/2$, $n = 0, 1, 2, ...$ the solution to (31) can be written in terms of the iterated error functions [6]. The case $n = 2$, imposing the boundary condition (27) with

$$H_0(t) = \left(H_0/\tau_r\right) t \tag{32}$$

gives

$$F(u) = 2\left(H_0/\tau_r\right)\left[\left(u^2 + 1/2\right)\operatorname{erfc}(u) - ue^{-u^2}/\sqrt{\pi}\right] \tag{33}$$

where $\operatorname{erfc}(u) = \frac{2}{\sqrt{\pi}} \int_u^\infty e^{-t^2} dt$ is the complementary error function. The surface electric field in this special case is thus given by

$$E_0\left(\left(H_0/\tau_r\right) t\right) = \left(H_0/\tau_r\right) \sqrt{\frac{4\mu t}{\pi\sigma}} \tag{34}$$

The total internal wall voltage V_{int} can be determined by integration of the surface electric field $E_0\left(H_0\left(t\right)\right)$ over the wall surface (say the bottom wall in z, for which the current is converging on the bolt) from the bolt hole to the point in Figure 4 where $V_{\max}$ is desired (there is also a multiplicative

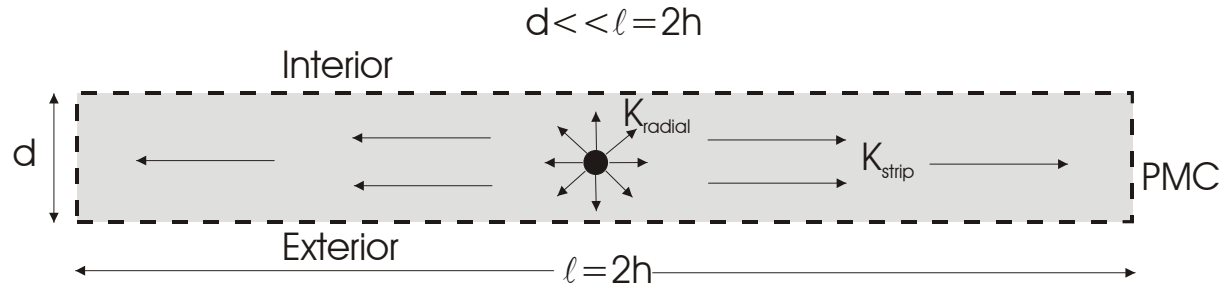

Figure 7. Approximate decomposition of current distribution into stripline and radial components when depth is much smaller than length.

factor of two because there are two walls of the slot) $\frac{1}{2}V_{int} = -\int_{C_{wall}} \underline{E}_0 \cdot \underline{d\ell}$. The current distribution is not disturbed by the finite wall conductivity since its influence on the distribution is identical to the external inductance (under the assumption that the planar solution can be used to relate the surface electric and magnetic fields). Note that $\underline{E}_0$ has the same direction as $\underline{K} = \underline{n} \times \underline{H}_0$ (where $\underline{n}$ points out of the metal) and that we can write the external (in the gap w) flux as $\Phi = \mu_0 w \int_{C_{wall}} \underline{H}_0 \cdot (\underline{n} \times \underline{d\ell}) = -\mu_0 w \int_{C_{wall}} (\underline{n} \times \underline{H}_0) \cdot \underline{d\ell} = -\mu_0 w \int_{C_{wall}} \underline{K} \cdot \underline{d\ell} = L_{\max} I = 2hL_{\max} K_z^{sc}$. Thus the electric field integration can be written in terms of the external inductance

$$\frac{1}{2}V_{int} = -\int_{C_{wall}} \underline{E}_0(K) \cdot \underline{d\ell} = -\frac{E_0(K_z^{sc})}{K_z^{sc}} \int_{C_{wall}} \underline{K} \cdot \underline{d\ell} = E_0(K_z^{sc}(t)) \frac{2h}{\mu_0 w} L_{\max}$$

$$= \frac{1}{\mu_0 w} L_{\max} \sqrt{\mu/\sigma} \frac{d^{1/2} I}{dt^{1/2}} \tag{35}$$

The special case of a linearly increasing current gives

$$\frac{1}{2}V_{int} = \sqrt{\frac{4\mu t}{\pi\sigma}} \frac{L_{\max}}{\mu_0 w} I_0/\tau_r \tag{36}$$

The use of the planar solution (28), (30), or (34) is only rigorously justified near the bolt hole if the radius a is much larger than the depth of penetration. At early times where the peak voltage occurs, this assumption is reasonable.

The fit (21), which is valid for the centered bolt $f = 0$, can be viewed as arising from a stripline flow of current in addition to a radial current flow near the bolt, as shown in Figure 7 and 8.

The surface current density (again $\underline{n} \times \underline{H}_0 = \underline{K}$ is the relation between the surface magnetic field and the surface current density) along the stripline is $K_x = -\frac{1}{d}\int_x^h K_z^{sc} dx = -\frac{1}{d}(h-x)K_z^{sc}$ and near the bolt is $K_\rho = -I/(2\pi\rho)$, where $I = 2hK_z^{sc}$. Therefore the voltage in the centered bolt case, is given by

$$\frac{1}{2}V_{int} = -\frac{E_0(K_z^{sc})}{K_z^{sc}} \int_{C_{wall}} \underline{K} \cdot \underline{d\ell} \approx E_0(K_z^{sc}(t)) \left[\frac{h}{\pi} \int_a^{b_{eff}} \frac{d\rho}{\rho} + \frac{1}{d} \int_0^h (h-x) dx \right]$$

$$= \left[\frac{1}{2\pi} \ln(b_{eff}/a) + \frac{1}{4}\frac{h}{d} \right] \sqrt{\mu/\sigma} \frac{d^{1/2} I}{dt^{1/2}} \tag{37}$$

where from (21) we take the effective outer radius of the radial current distribution to be

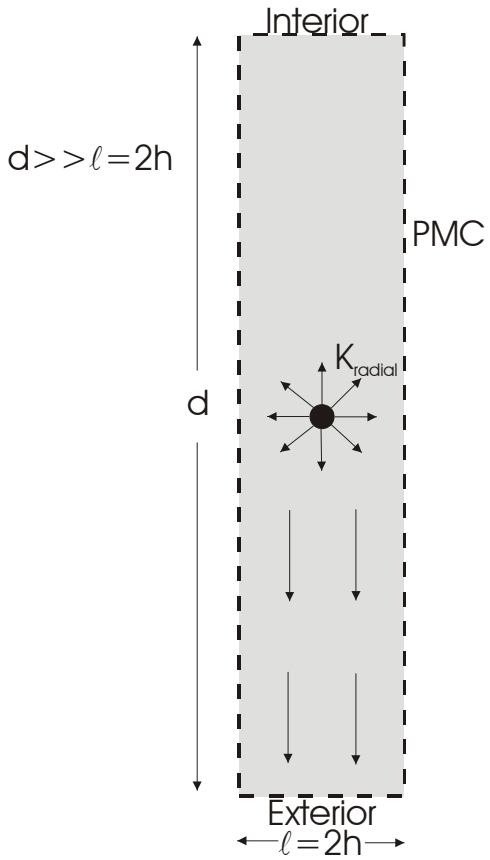

Figure 8. Approximate decomposition of current distribution into stripline and radial components when depth is much larger than length.

$$b_{eff} \approx \frac{hd/(2\pi)}{h + d/2} \tag{38}$$

The value of this effective radius obviously results from the actual transition of the current from a radial distribution to that of a stripline. Nevertheless the superposition of radial and stripline current distributions is a useful approximate pictorial representation of the voltage. The linearly rising current waveform gives

$$\frac{1}{2}V_{int} \approx \left[\frac{1}{2\pi}\ln(b_{eff}/a) + \frac{1}{4}\frac{h}{d}\right] 2\sqrt{\frac{\mu t}{\pi\sigma}}\,(I_0/\tau_r) \tag{39}$$

4 FERROMAGNETIC WALL VOLTAGE

We consider here the simplifying assumption of a step hysteresis function such that

$$B = B_s \mathrm{sgn}(H) \tag{40}$$

Assuming that $H > 0$ the depth of saturation is [7], [8]

$$z_0(t) = \sqrt{\frac{2}{\sigma B_s}\int_0^t H_0(\tau)d\tau} \tag{41}$$

The surface electric field is [8]

$$E_0\left(H_0\left(t\right)\right) = B_s\frac{\partial}{\partial t}z_0(t) = \frac{\sqrt{B_s/(2\sigma)}H_0(t)}{\sqrt{\int_0^t H_0(\tau)d\tau}} \tag{42}$$

The special case of a linearly increasing current (32) gives the surface electric field

$$E_0\left(\left(H_0/\tau_r\right)t\right) = \sqrt{\left(H_0/\tau_r\right)B_s/\sigma} \tag{43}$$

The total voltage is again found by integration of the surface electric field from the bolt hole to the point where the slot voltage is desired. Unfortunately in the nonlinear case the finite wall conductivity influences the current distribution in a manner different than the external inductance. Thus the current distribution is changed somewhat and the external inductive contribution to the total voltage is also changed. The actual current distribution can be rigorously determined by constructing a nonlinear resistive-inductive network for the region in Figure 4.

A simple approximate answer in the nonlinear case, with centered bolt $f = 0$, can be obtained by the following consideration. The combination of stripline current distribution and radial bolt hole current distribution is still a reasonable model for the voltage contributions in the nonlinear case; the only question, is what to use for the effective transition radius b_{eff}. This question can be answered rigorously by the numerical network solution mentioned in the preceding paragraph. However, to obtain a rough approximation for the voltage, it seems reasonable to use the linear equivalent radius (38). With this approximation the external voltage contribution remains the same as discussed previously (23) and (25). The surface electric field, (42) or (43), depends on the square root of the surface current amplitude. Taking the current densities to be $K_x = -\frac{1}{d}\int_x^h K_z^{sc}dx = -\frac{1}{2hd}(h-x)I$, $K_\rho = -I/(2\pi\rho)$, using (42), we obtain

$$\frac{1}{2}V_{int} = -\int_{C_{wall}} \underline{E}_0(K)\cdot \underline{d\ell} \approx \sqrt{\frac{B_s}{2\sigma}}\frac{I(t)}{\sqrt{\int_0^t I(\tau)d\tau}}\left[\frac{1}{\sqrt{2hd}}\int_0^h \sqrt{h-x}dx + \frac{1}{\sqrt{2\pi}}\int_a^{b_{eff}}\frac{d\rho}{\sqrt{\rho}}\right]$$

$$\approx \sqrt{\frac{B_s}{\sigma}}\frac{I(t)}{\sqrt{\int_0^t I(\tau)d\tau}}\left[\frac{1}{3\sqrt{d}}h + \frac{1}{\sqrt{\pi}}\left(\sqrt{b_{eff}}-\sqrt{a}\right)\right] \tag{44}$$

The linearly rising current (24) gives

$$\frac{1}{2}V_{int} \approx \sqrt{\frac{2B_sI_0}{\tau_r\sigma}}\left[\frac{1}{3\sqrt{d}}h + \frac{1}{\sqrt{\pi}}\left(\sqrt{b_{eff}}-\sqrt{a}\right)\right] \tag{45}$$

It is interesting to note that the appearance of the bolt hole radius a rather than some effective radius (to account for two dimensional axisymmetric diffusion near the bolt when a is not large compared to the penetration depth) is less critical here than in the linear case, since the surface electric field varies as $O\left(1/\sqrt{\rho}\right)$ rather than as $O(1/\rho)$ in the linear case.

5 BOLT AND HOLE CONTRIBUTION

We assume that the bolt with radius $a_{bolt} < a$ is centered in the bolt hole. The external inductance associated with the clearance is thus given by

$$L_{bolt} \approx \frac{\mu_0 s_{bolt}}{2\pi}\ln\left(a/a_{bolt}\right) \tag{46}$$

where s_{bolt} is the length of the bolt shaft and we will assume it includes both sides of the slot.

The internal bolt and hole voltage is determined assuming that the early time penetration distance (where the peak joint voltage occurs) is much less than the bolt radius a_{bolt}. The result in either the linear case or the ferromagnetic case can be written as

$$V_b \approx s_{bolt}E_0\left(H_0(t)\right) \tag{47}$$

where $E_0\left(H_0(t)\right)$ is given by (30) in the linear case and by (42) in the ferromagnetic case, and in both cases $H_0(t) = I(t)/(2\pi a_{bolt})$. The linearly rising current waveform (24) yields

$$V_b \approx \sqrt{\frac{4\mu t}{\pi\sigma}}\left(\frac{s_{bolt}}{2\pi a_{bolt}}\right)I_0/\tau_r \tag{48}$$

in the linear case and

$$V_b \approx s_{bolt}\sqrt{\frac{B_sI_0/\tau_r}{\sigma\left(2\pi a_{bolt}\right)}} \tag{49}$$

in the ferromagnetic case.

The internal voltage resulting from the bolt hole is the same as (47), (48), and (49) except that the bolt radius a_{bolt} is replaced by the bolt hole radius a, the bolt shaft length s_{bolt} is replaced by the length of the bolt hole $s_{hole} = s_{bolt} - w \approx s_{bolt}$, and the material properties of the bolt hole material are used.

6 FERROMAGNETIC WALL VOLTAGE FOR VERY LARGE DRIVE CURRENT

If the drive current is very large (for example, for a small number of slots around the circumference) we must account for the flux behind the saturation front in the wall electric field. This gives a wall electric field

$$E_0(t) = B_s \frac{\partial}{\partial t} z_0 + \frac{\partial}{\partial t}\left(\frac{1}{2} z_0 \mu_0 H_0(t)\right)$$

$$z_0(t) = \sqrt{\frac{2/\sigma}{B_s \frac{1}{3}\mu_0 H_0(t)} \int_0^t H_0(\tau)\, d\tau}$$

A linearly rising magnetic field gives

$$E_0(t) = B_s \frac{z_0}{t}(1 - \tau_0/t) + \mu_0 (H_0/\tau_r)\, t \frac{z_0}{t}\left(1 - \frac{1}{2}\tau_0/t\right)$$

$$\tau_0(t) = \frac{1}{6}\mu_0 \sigma z_0^2$$

$$z_0(t) = t\sqrt{\frac{(H_0/\tau_r)/\sigma}{B_s + \frac{1}{3}\mu_0 (H_0/\tau_r)\, t}}$$

The peak can be approximated by replacing t by τ_r

$$E_0 = B_s \frac{z_0}{\tau_r}(1 - \tau_0/\tau_r) + \mu_0 H_0 \frac{z_0}{\tau_r}\left(1 - \frac{1}{2}\tau_0/\tau_r\right)$$

$$\tau_0 = \frac{1}{6}\mu_0 \sigma z_0^2$$

$$z_0 = \tau_r \sqrt{\frac{(H_0/\tau_r)/\sigma}{B_s + \frac{1}{3}\mu_0 H_0}}$$

7 ESTIMATE FOR PEAK VOLTAGE

The quantity of practical interest is the peak joint voltage. Figure 9 sketches a simple procedure for estimating this peak voltage.

The lightning current is fit with a linear ramp extending from the initial instant to the rise time τ_r of the actual waveform, such that the peak amplitude is arrived at and the maximum slope is well approximated. The external inductive contribution to the voltage (including both the slot and bolt clearance hole) resulting from this linear current is constant. The nonlinear ferromagnetic contribution is also constant (for both the slot walls, the bolt, and bolt hole). The linear internal diffusive contribution varies as $O\left(\sqrt{t}\right)$ for the linear current waveform. Thus to obtain an estimate for the peak voltage we evaluate the linear diffusive contribution at time

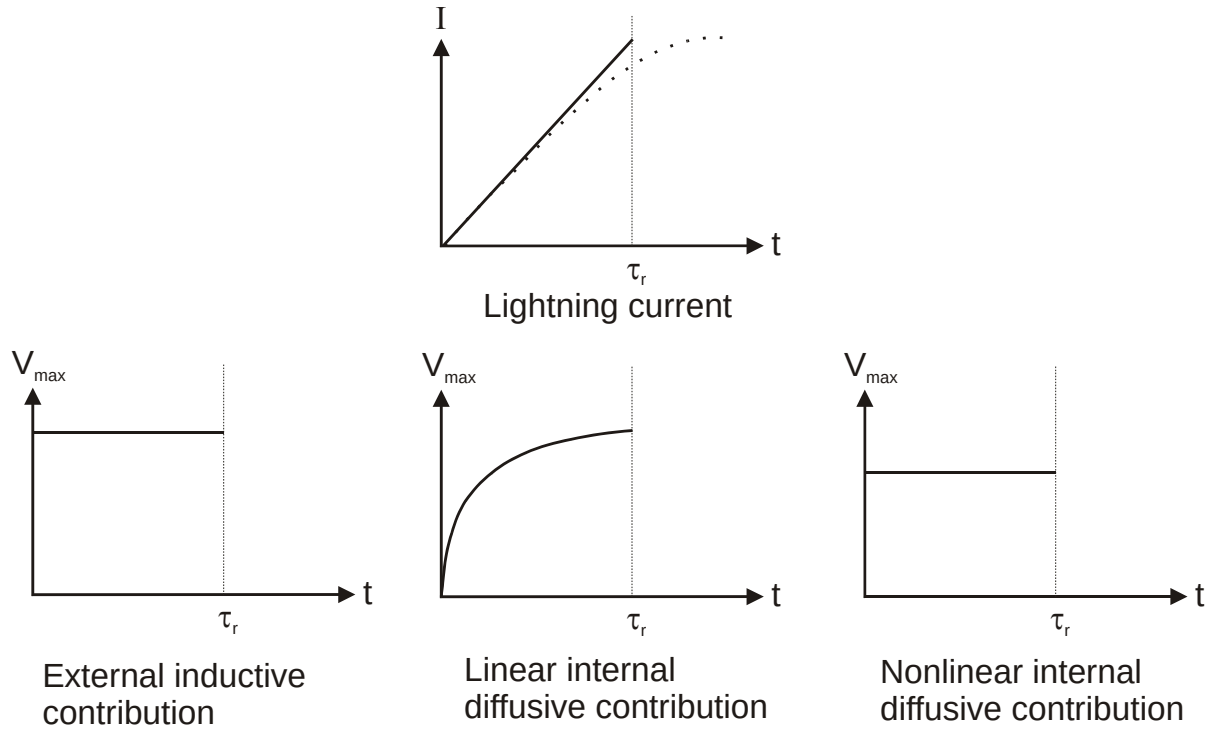

Figure 9. Approximate linear ramp fit of lightning current waveform and the resulting time behavior of the various parts of the joint voltage.

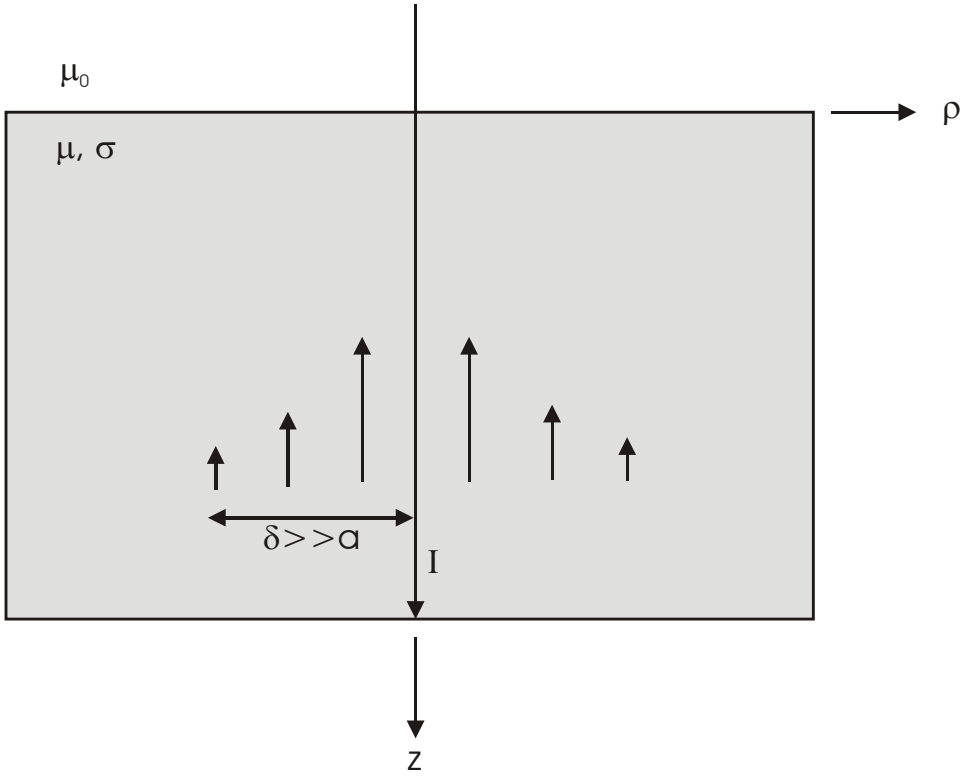

Figure 10. Illustration of bolt current when the depth of penetration δ is large compared to the bolt hole radius and the current is induced by a filament approximation to the bolt.

$$t = \tau_r \tag{50}$$

Note that the external inductive voltage and internal nonlinear voltages will fall off (from the constant value) as the actual current waveform deviates from the linear fit; the internal linear voltage will also decrease from the $O\left(\sqrt{t}\right)$ behavior near the peak of the actual current waveform.

8 LINEAR BOLT HOLE VOLTAGE

It is of interest to consider what happens to the effective bolt hole radius when the depth of penetration is large compared to the actual hole radius. Simplification of the problem is accomplished by shrinking the bolt hole radius to zero but inducing the magnetic field in the conductor by an axial current filament as shown in Figure 10.

We first ignore the interface at $z = 0$ and take the filament (and the conducting medium) to be of infinite extent. The problem is then independent of φ and z. Eliminating the magnetic field in the Laplace transform of Maxwell's equations $\nabla \times \underline{E} = -s\mu\underline{H}$ (assuming $\underline{H}\,(t=0) = 0$) and $\nabla \times \underline{H} = \underline{J} + \sigma\underline{E}$, and using $J_z = I\delta(\rho)/(2\pi\rho)$, thus gives $\left[\frac{1}{\rho}\frac{\partial}{\partial\rho}\left(\rho\frac{\partial}{\partial\rho}\right) - s\mu\sigma\right] E_z = s\mu I\delta(\rho)/(2\pi\rho)$. The solution which vanishes as $\rho \to \infty$ can be written as

$$E_z^e = -s\mu\frac{I}{2\pi}K_0\left(\rho\sqrt{s\mu\sigma}\right) \tag{51}$$

where the superscript e denotes the fact that this one dimensional part of the solution satisfies a perfect electric conductor (PEC) boundary condition at $z = 0$, and $K_n(x)$ is the modified Bessel function of the second king of order n. Using $-\frac{\partial}{\partial\rho}E_z = -s\mu H_\varphi$ gives

$$H_\varphi^e = \sqrt{s\mu\sigma}\frac{I}{2\pi}K_1\left(\rho\sqrt{s\mu\sigma}\right) \tag{52}$$

The total field satisfies the boundary condition

$$H_\varphi^{tot} = H_\varphi^e + H_\varphi = I/(2\pi\rho)\,,\ z = 0 \tag{53}$$

where the boundary contribution H_φ is independent of φ and satisfies

$$\left(\nabla^2 - s\mu\sigma - 1/\rho^2\right)H_\varphi = 0 \tag{54}$$

The integral (Hankel) transform solution can be taken as

$$H_\varphi = \int_0^\infty \alpha A(\alpha)J_1(\alpha\rho)e^{-z\sqrt{s\mu\sigma+\alpha^2}}d\alpha \tag{55}$$

where $J_1(x)$ is the Bessel function of the first kind of order unity. Applying the boundary condition (53) and using the orthogonality of the Hankel transform gives

$$A(\alpha) = \int_0^\infty \rho J_1(\alpha\rho)\left[\frac{I}{2\pi\rho} - \sqrt{s\mu\sigma}\frac{I}{2\pi}K_1\left(\rho\sqrt{s\mu\sigma}\right)\right]d\rho = \frac{Is\mu\sigma}{2\pi\alpha(s\mu\sigma+\alpha^2)} \tag{56}$$

The electric field is determined by means of $E_z = \frac{1}{\sigma}\left(\frac{\partial}{\partial\rho} + \frac{1}{\rho}\right)H_\varphi$ and $E_\rho = -\frac{1}{\sigma}\frac{\partial}{\partial z}H_\varphi$. The total electric field requires the addition of the one dimensional solution (51). Because the contribution to the total voltage of the one dimensional solution is usually the dominant part, it is convenient to determine the exact one dimensional solution to the bolt hole geometry shown in Figure 11.

The boundary condition at $\rho = a$ is $H_\varphi^e(a) = I/(2\pi a)$. The electric field is thus

$$E_z^e = -\frac{I}{2\pi a}\sqrt{s\mu/\sigma}K_0\left(\rho\sqrt{s\mu\sigma}\right)/K_1\left(a\sqrt{s\mu\sigma}\right) \tag{57}$$

We require only the values of $E_z(\rho = 0)$ and $E_\rho(z = 0)$ of the difference field (we can approximate the difference field E_z at $\rho = 0$ instead of at $\rho = a$), which can be written as

$$E_z(0,z) = \frac{s\mu I}{2\pi}\int_0^\infty \frac{\alpha}{s\mu\sigma+\alpha^2}e^{-z\sqrt{s\mu\sigma+\alpha^2}}d\alpha = \frac{s\mu I}{2\pi}E_1\left(z\sqrt{s\mu\sigma}\right) \tag{58}$$

$$E_\rho(\rho,0) = \frac{s\mu I}{2\pi}\int_0^\infty J_1(\alpha\rho)\frac{d\alpha}{\sqrt{s\mu\sigma+\alpha^2}} = \frac{I}{2\pi\rho}\sqrt{s\mu/\sigma}\left(1 - e^{-\rho\sqrt{s\mu\sigma}}\right) \tag{59}$$

where $E_1(z) = \int_z^\infty e^{-u}du/u$ is the exponential integral. The one dimensional part of the total voltage V^{tot} is

$$V^e = -s_{hole}E_z^e(a) = s_{hole}\frac{I}{2\pi a}\sqrt{s\mu/\sigma}K_0\left(a\sqrt{s\mu\sigma}\right)/K_1\left(a\sqrt{s\mu\sigma}\right) \tag{60}$$

The difference voltage (for a single wall) consists of the two contributions

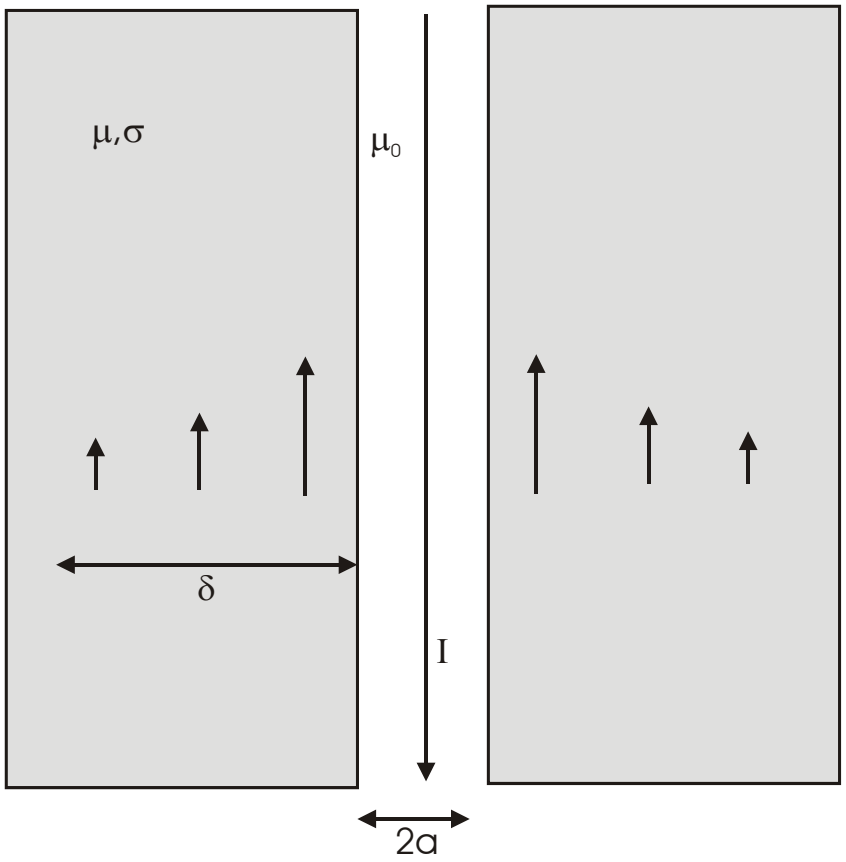

Figure 11. Exact one dimensional illustration of bolt current, when the depth of penetration δ is large compared to the bolt hole radius, used to obtain the dominant part of the bolt impedance.

$$V_{\rho_0} = \int_0^{\rho_0} E_\rho(\rho, 0) d\rho + \int_\infty^0 E_z(0, z) dz \tag{61}$$

where we have let $s_{hole} \to \infty$ in the second integral since the metal is assumed to be many skin depths thick. The distance ρ_0 is assumed to be many skin depths in size so that the current field is one dimensional beyond this radius; thus the linear wall electric field, (30) or (34), is valid. The integrations in (61) can be carried out as

$$V_{\rho_0} \sim \frac{I}{2\pi} \sqrt{s\mu/\sigma} \left[\ln\left(\rho_0 \sqrt{s\mu\sigma}\right) + \gamma' - 1 \right] \tag{62}$$

where $\gamma' \approx 0.5772$ is Euler's constant and the term $\frac{1}{2\pi}\sqrt{s\mu/\sigma} E_1(\rho_0\sqrt{s\mu\sigma})$ has been neglected. The -1 in brackets in (62) results from the second integral in (61). If we replace the bolt hole contribution (47) (with $s_{bolt} \to s_{hole}$ and $a_{bolt} \to a$) by the inverse transform of (60), then we can lump the inverse transform of the correction (62) entirely with the slot wall voltage (35) or (36). The field contribution to the wall voltage from the vicinity of the large distance (compared to the skin depth) $\rho = \rho_0$ was treated correctly by the previous planar arguments (it is only when ρ is of the order of the skin depth that the planar arguments fail). Thus we can subtract from the previous result, (35) or (36), the planar transform contribution $\frac{I}{2\pi}\sqrt{s\mu/\sigma}\ln(\rho_0/a)$ and add the inverse transform of (62). Alternatively we can add to (35) or (36) the inverse transform of the voltage correction

$$\frac{1}{2}\Delta V = V_{\rho_0} - \frac{I}{2\pi}\sqrt{s\mu/\sigma}\ln(\rho_0/a) = \frac{I(s)}{2\pi}\sqrt{s\mu/\sigma}\left[\ln\left(a\sqrt{s\mu\sigma}\right) + \gamma' - 1\right] \tag{63}$$

For linearly rising current (24) $I(s) = I_0/\left(s^2\tau_r\right)$. Noting the inverse Laplace transform pairs $s^{-\alpha} \Leftrightarrow t^{\alpha-1}/\Gamma(\alpha)$ and $s^{-\alpha}\ln(s) \Leftrightarrow t^{\alpha-1}\left[\psi(\alpha) - \ln(t)\right]/\Gamma(\alpha)$, where $\alpha > 0$ and $\psi(\alpha)$ is the digamma function [6], thus gives

$$\frac{1}{2}\Delta V = \frac{I_0/\tau_r}{2\pi}\sqrt{\frac{\mu t}{\pi\sigma}}\left[2\ln\left(a\sqrt{\frac{\mu\sigma}{4t}}\right) + \gamma'\right] = 2\sqrt{\frac{\mu t}{\pi\sigma}}\left(I_0/\tau_r\right)\frac{1}{2\pi}\ln\left(a/a_{eff}\right) \tag{64}$$

where the effective bolt hole radius is

$$a_{eff} = \sqrt{\frac{4te^{\gamma'}}{\mu\sigma}} \tag{65}$$

Combining (64) with (36) or (39) gives

$$\frac{1}{2}V_{int} + \frac{1}{2}\Delta V \approx \left[\frac{1}{2\pi}\ln(b_{eff}/a_{eff}) + \frac{1}{4}\frac{h}{d}\right] 2\sqrt{\frac{\mu t}{\pi\sigma}}\left(I_0/\tau_r\right) \tag{66}$$

where the assumption is that $b_{eff} >> a_{eff} >> a$. The inverse transform of the one dimensional bolt hole voltage (60) is complicated. However if (60) is expanded for $a\sqrt{s\mu\sigma} << 1$ we have

$$V^e \sim -s_{hole}\frac{s\mu I}{2\pi}\left[\ln\left(\frac{a}{2}\sqrt{s\mu\sigma}\right) + \gamma'\right] \tag{67}$$

The inverse transform for the linearly rising current thus gives the additional one dimensional bolt hole voltage

$$V^e \sim \left(I_0/\tau_r\right) s_{hole}\frac{\mu}{2\pi}\ln\left(a_{eff}/a\right) \tag{68}$$

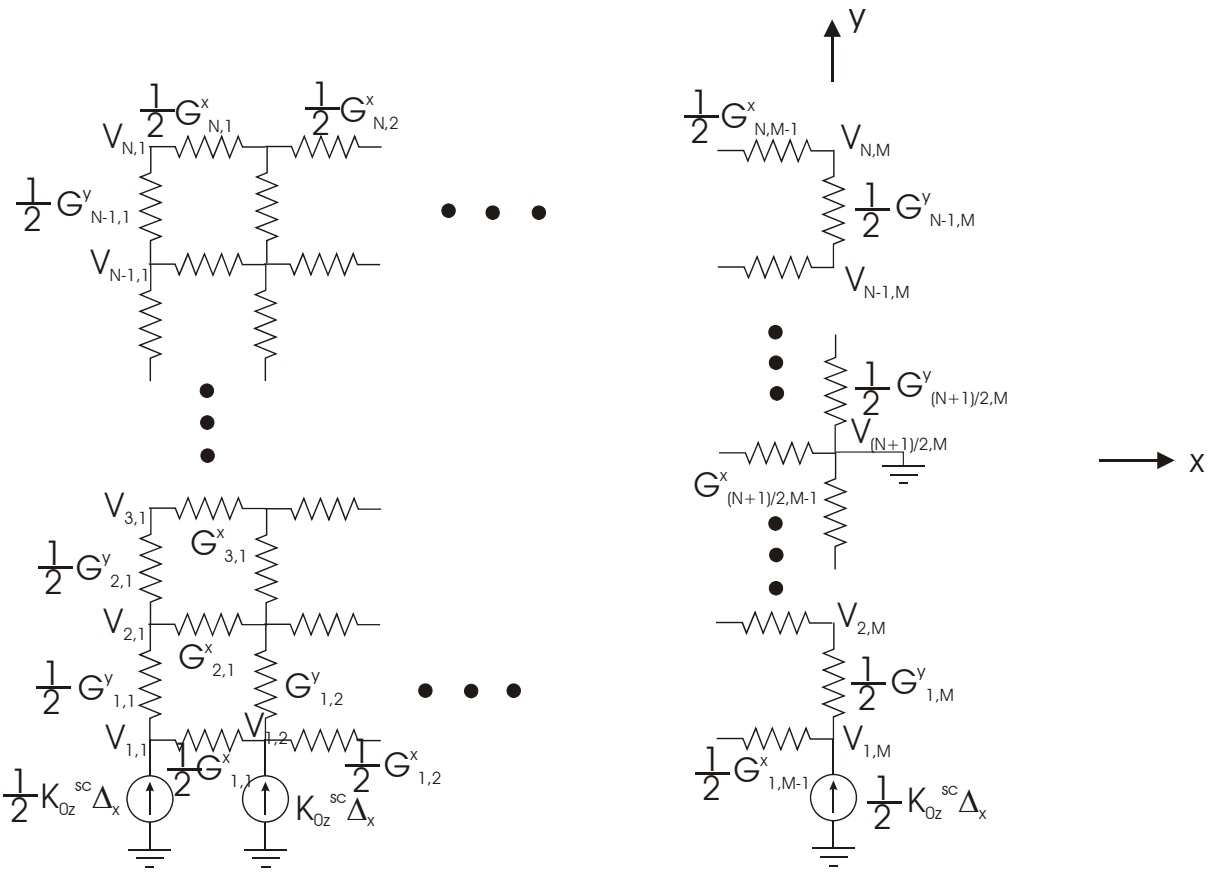

Figure 12. Nonlinear resistive network used to model ferromagnetic wall voltage.

The internal bolt voltage in this deep penetration limit is not (47) or (48), but is instead given by

$$V_b \sim s_{bolt} I(s) \left(\frac{1}{\pi a_{bolt}^2 \sigma} + s \frac{\mu}{8\pi} \right) \tag{69}$$

The linearly ramp current thus results in

$$V_b \sim s_{bolt} (I_0/\tau_r) \left(\frac{t}{\pi a_{bolt}^2 \sigma} + \frac{\mu}{8\pi} \right) \tag{70}$$

There are of course also corrections arising from the bolt head region (which would require the detailed geometry of the bolt head region to be specified) in this limit.

9 FERROMAGNETIC BOLT HOLE AND WALL VOLTAGE

The estimate given in Section 4 for the nonlinear wall voltage is now checked by a numerical calculation. Figure 12 shows a nonlinear resistive network for the ferromagnetic wall (exploiting symmetry about the bolt, which is assumed to be centered in the slot, including $f = 0$).

The gap w is taken to be small compared to the depth of penetration in the metal walls of the slot, so the current distribution is determined exclusively by the nonlinear wall admittance. The bolt and hole radii are taken to be zero (the ground point $V_{(N+1)/2,M} = 0$, where N is odd). We again take the current to rise linearly with time (32) so that the electric field on the wall is given by (43). The wall admittance is thus a nonlinear conductance given by

$$\underline{K}_0/\underline{E}_0 = G(K_0) = \sqrt{\tau_r \sigma K_0/B_s} \tag{71}$$

where the total surface current amplitude ($K = (K_0/\tau_r)\, t$) is $\underline{K}_0 = \underline{n} \times \underline{H}_0$ and the unit outward normal is, say, $\underline{n} = \underline{e}_z$. The lumped conductance spacing in the x direction of Figure 12 is taken as $\Delta_x = h/(M-1)$ and in the y direction as $\Delta_y = d/(N-1)$. Thus the lumped current sources have current $K_{0z}^{sc}\Delta_x$ (one half this value at the half cell ends $m = 1, M$), where $K_{0z}^{sc} = I_0/(2h)$, and the circuit currents are $I^x = \Delta_y K_{0x}$ and $I^y = \Delta_x K_{0y}$. The lumped circuit conductances are therefore

$$G^x(K_0) = \frac{K_{0x}\Delta_y}{E_{0x}\Delta_x} = \frac{\Delta_y}{\Delta_x}\sqrt{\tau_r \sigma K_0/B_s} \tag{72}$$

$$G^y(K_0) = \frac{K_{0y}\Delta_x}{E_{0y}\Delta_y} = \frac{\Delta_x}{\Delta_y}\sqrt{\tau_r \sigma K_0/B_s} \tag{73}$$

where the total surface current density is related to the circuit currents by means of $K_0 = \sqrt{(I^x/\Delta_y)^2 + (I^y/\Delta_x)^2}$. On the boundary of the grid we take one half of the conductance values (72) or (73).

The update of the nonlinear conductances was carried out by the following procedure. At a nodal point where the voltage is defined as $V_{n,m}$ we determine the currents in the x direction $I_{n,m}^{-x} = (V_{n,m-1} - V_{n,m})\, G_{n,m-1}^x$ and $I_{n,m}^{+x} = (V_{n,m} - V_{n,m+1})\, G_{n,m}^x$ and y direction $I_{n,m}^{-y} = (V_{n-1,m} - V_{n,m})\, G_{n-1,m}^y$ and $I_{n,m}^{+y} = (V_{n,m} - V_{n+1,m})\, G_{n,m}^y$ on either side of the nodal point. Averages are then taken $I_{n,m}^x = \left(I_{n,m}^{-x} + I_{n,m}^{+x}\right)/2$ and $I_{n,m}^y = \left(I_{n,m}^{-y} + I_{n,m}^{+y}\right)/2$ (on the boundary one of the currents $I_{n,m}^{\pm x}$ or $I_{n,m}^{\pm y}$ is set to zero) and the total surface current is found as $K_0^{n,m} = \sqrt{(I_{n,m}^x/\Delta_y)^2 + (I_{n,m}^y/\Delta_x)^2}$. Each of the four conductances surrounding the node $V_{n,m}$ are then thought of as consisting of two conductances in series, the ones terminating on the node $V_{n,m}$ having the values $2G^x\left(K_0^{n,m}\right)$ or $2G^y\left(K_0^{n,m}\right)$. This is done for each node and the sets of two series conductances are combined to form the single conductances $G_{n,m}^x$ and $G_{n,m}^y$ as shown in Figure 12. Another linear system solution is then found and the iteration is repeated.

The circuit equations to be solved from Figure 12 are

$$0 = (V_{n,m} - V_{n,m+1})\left(1 - \frac{1}{2}\delta_{n,1} - \frac{1}{2}\delta_{n,M}\right) G_{n,m}^x + (V_{n,m} - V_{n+1,m})\left(1 - \frac{1}{2}\delta_{m,1} - \frac{1}{2}\delta_{m,M}\right) G_{n,m}^y$$

$$+ (V_{n,m} - V_{n-1,m})\left(1 - \frac{1}{2}\delta_{m,1} - \frac{1}{2}\delta_{m,M}\right) G_{n-1,m}^y + (V_{n,m} - V_{n,m-1})\left(1 - \frac{1}{2}\delta_{n,1} - \frac{1}{2}\delta_{n,N}\right) G_{n,m-1}^x$$

$$-K_{0z}^{sc}\Delta_x \delta_{n,1}\left(1 - \frac{1}{2}\delta_{m,1} - \frac{1}{2}\delta_{m,M}\right)$$

$$V_{(N+1)/2,M} = 0 \tag{74}$$

where terms with indices off the grid are taken to be zero. These nonlinear equations were solved by simple

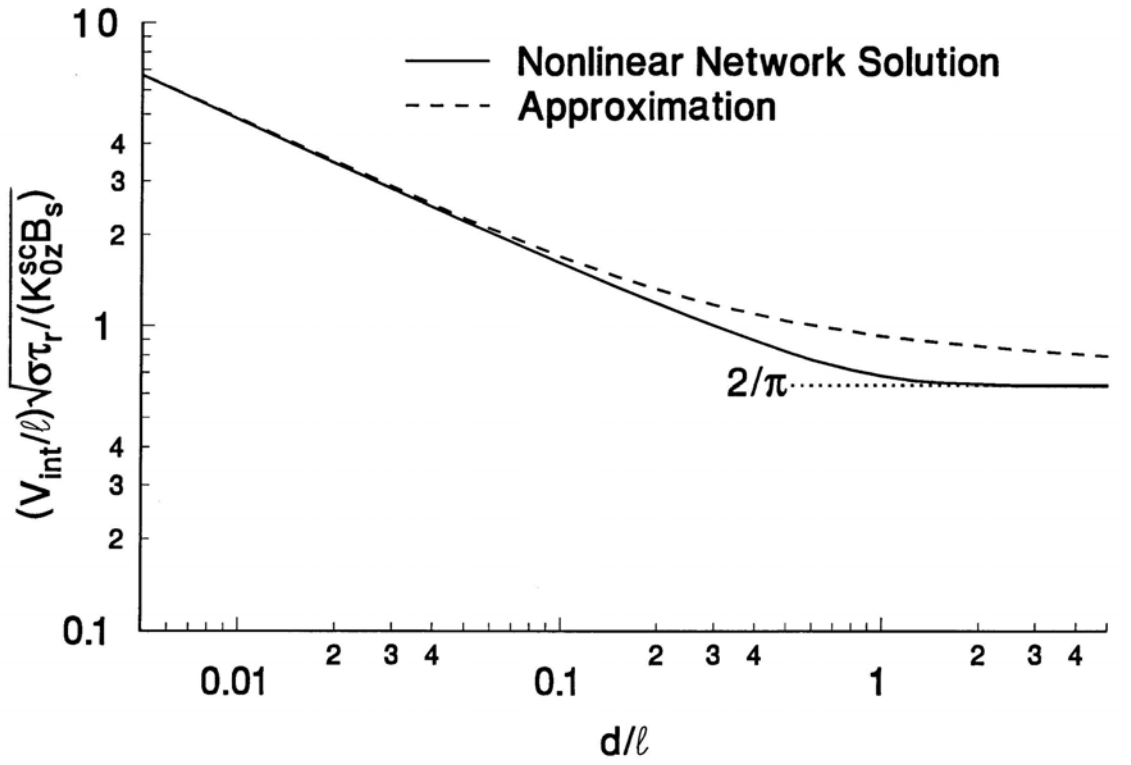

Figure 13. Scaled ferromagnetic wall voltage from solution of nonlinear resistive network.

iteration evaluating the arguments of the conductances at the previous iteration step. The initial guess was taken as $K_0^{n,m} = |K_{0z}^{sc}|$ and ten iterations were applied. The maximum interior voltage on a single wall was determined

$$\frac{1}{2}V_{int} = V_{N,1} \tag{75}$$

The ratio of unknowns was taken to maintain approximately square cells $(M-1)/(N-1) \approx h/d$. Extrapolation to the limit $N \to \infty$ was used by taking the desired result to be given by $V = V_{N,1} + \alpha/(N-1)$. The scaling of the results as

$$\frac{\frac{1}{2}V_{int}}{hE_0(K_{0z}^{sc})} = \frac{\frac{1}{2}(V_{int}/h)}{G(K_{0z}^{sc})/K_{0z}^{sc}} = \frac{\frac{1}{2}(V_{int}/h)}{\sqrt{K_{0z}^{sc}B_s/(\tau_r\sigma)}} = (V_{int}/\ell)\sqrt{\tau_r\sigma/(K_{0z}^{sc}B_s)} \tag{76}$$

allows a single curve, as a function of d/ℓ, to describe the results for any set of parameters. Figure 13 gives the scaled voltage and the approximation (45) with $a = 0$.

Although there is some error in the approximation, notice that it bounds the numerical result for all d/ℓ. The approximation actually gives the value $2/\pi$ as $d/\ell \to \infty$ which is the asymptote of the numerical solution shown on the graph. For small values of d/ℓ the stripline contribution dominates, and again the nonlinear circuit result approaches the approximation. The use of the linear value for b_{eff} (38) thus provides a useful estimate (and bound) for the nonlinear wall voltage. The external inductive voltage (resulting from a nonnegligible gap w) can thus be consistently added to this approximation as discussed previously.

The bolt voltage in this deep penetration limit is given by (69) or (70), with $\mu \to \mu_0$ assuming the material is saturated. The ferromagnetic bolt hole voltage for deep penetration is now determined referring again to the geometry of Figures 10 and 11. We assume that the material is saturated out to a distance $\rho_0(t)$ which is large compared to a (thus we ignore the radius a and assume the z directed bolt current I exists along a filament at $\rho = 0$). We ignore the linear diffusion in the saturated region and solve the static limit of (54) with no z dependence

$$\left(\frac{\partial^2}{\partial\rho^2} + \frac{1}{\rho}\frac{\partial}{\partial\rho} - \frac{1}{\rho^2}\right) H_\varphi \approx 0 \tag{77}$$

The boundary conditions are [8]

$$H_\varphi = \frac{I}{2\pi\rho}\,,\ \rho \to 0 \tag{78}$$

$$H_\varphi = 0\,,\ \rho = \rho_0(t) \tag{79}$$

The solution is thus

$$H_\varphi = \frac{I}{2\pi\rho}\left[1 - \rho^2/\rho_0^2(t)\right]\,,\ 0 < \rho < \rho_0(t)$$

$$= 0\,,\ \rho > \rho_0(t) \tag{80}$$

The electric field in the saturated region using $E_z = \frac{1}{\sigma}\left(\frac{\partial}{\partial\rho} + \frac{1}{\rho}\right) H_\varphi$ is

$$E_z = -\frac{I}{\pi\sigma\rho_0^2(t)} \tag{81}$$

Applying Faraday's law $\oint_C \underline{E}\cdot\underline{d\ell} = -\frac{\partial}{\partial t}\int_S \underline{B}\cdot\underline{n}\,dS$ to a fixed contour about the saturation front at $\rho = \rho_0(t)$ gives [8]

$$E_z = -B_s\frac{\partial}{\partial t}\rho_0(t) \tag{82}$$

Setting (81) and (82) equal, and taking $\rho_0(t) \to 0$ when $t = 0$ as the initial condition, determines the saturation front location

$$\rho_0(t) = \left[\frac{3}{\pi\sigma B_s}\int_0^t I(\tau)\,d\tau\right]^{1/3} \tag{83}$$

The bolt hole voltage is thus

$$V^e = -s_{hole}E_z = s_{hole}(\pi\sigma)^{-1/3} I(t) \Big/ \left[\frac{3}{B_s}\int_0^t I(\tau)\,d\tau\right]^{2/3} \tag{84}$$

The linearly rising current gives

$$\rho_0(t) = \left[\frac{3}{2\pi\sigma B_s}(I_0/\tau_r)\,t^2\right]^{1/3} \tag{85}$$

$$V^e = s_{hole}\left(\frac{4I_0}{9\pi\sigma\tau_r B_s^2 t}\right)^{1/3} \tag{86}$$

Note that if (78) is replaced by the exact condition $H_\varphi(\rho = a) = I/(2\pi a)$ (keeping the small distance a in the problem), then the magnetic field (80) is replaced by $H_\varphi = \frac{I}{2\pi\rho}\left(\frac{\rho_0^2-\rho^2}{\rho_0^2-a^2}\right)$, the electric field (81) is replaced by $E_z = -\frac{I}{\pi\sigma\left(\rho_0^2-a^2\right)}$, and the equation for the radial penetration depth is $\rho_0^3 - 3a^2\rho_0 + 2a^3 = \frac{3}{\pi\sigma B_s}\int_0^t I(\tau)\,d\tau$.

10 CONCLUSIONS

Lightning current excitation of bolted joints was addressed by the construction of simple external inductive and internal diffusive models of the joint. Symmetric drive conditions were assumed so a single slot (and bolt) could be considered alone. This also provides the worst case voltage (for a given uniform current density per slot) under asymmetric exterior current drives and is thus the natural bounding case to examine. The slot width is assumed to be sufficiently small compared to the slot length and depth that we can treat the openings of the slot to the interior and exterior of the shield as open circuits (very large exterior inductive loads).

The external transfer inductance (which gives the maximum interior slot voltage given the exterior slot drive current) was estimated in (16). A simple fit for the case when the bolt is centered in the slot is given by (22), or for small bolt radius by (21). The voltage resulting from this external inductance is thus given by (23), or for a linear ramp lightning current (24) by (25).

The internal linear wall diffusive contribution to the slot voltage was estimated by first determining the surface electric field on a half space conductor (28) or (30), or for a linear ramp lightning current by (34). This was integrated along the wall to find the total wall voltage contribution (35), or for linear ramp lightning current (36). It was remarked that the current distribution can be considered as having two parts: a stripline part with a uniform (in depth) Cartesian current distribution, and a radial part at the bolt. Using the effective radial transition radius (38) to truncate the integration of the radial current distribution, gives the nearly same external inductance and internal wall voltage, (37) or (39), as the rigorous expressions, in the linear wall case.

The ferromagnetic nonlinear wall voltage was addressed by assuming a step function hysteresis function for the material (40). The surface electric field on a half space was then given as (42), or for linear ramp current excitation as (43). The previous discussion of the two components of the current distribution (stripline and radial components) was then used to give a rough estimate for the nonlinear wall voltage (44), or for the linear ramp current (45).

The additional voltage resulting from a gap around the bolt hole was next given. The external bolt inductance is given by (46). The bolt voltage internal to the metal (and bolt hole voltage, which must also be added by replacement of the bolt radius by the bolt hole radius and bolt length by bolt hole length in these formulas) is given by (47). The linear ramp current waveform gives (48) for the linear wall material and (49) for the ferromagnetic wall material.

A simple estimate for the peak joint voltage was discussed. The early time linear ramp lightning current results in constant external inductive voltages as well as constant internal ferromagnetic wall voltages; the linear wall voltage, however, varies as the square root of the time. Evaluation of the linear wall voltage at the lightning current rise time (50) and addition of the other constant voltage contributions thus yields a

useful estimate of the peak joint voltage.

The previous calculations assume the early time penetration depth into the conductor to be small compared to the bolt hole and bolt radii. The next section considers the effective bolt hole radius when the depth of penetration is large compared to the bolt hole radius. The correction to the linear wall voltage is given in the Laplace domain by (63). An effective bolt hole radius (65) is determined for the linear ramp current and used in the linear wall voltage. The contribution from the bolt hole itself in this limit is (60) or (67) in the Laplace domain, or (68) for linear ramp current. The bolt voltage in this deep penetration limit is given by (69) in the Laplace domain and by (70) for linear ramp current.

The final section gives a more rigorous estimate of the wall voltage in the ferromagnetic case by means of a nonlinear resistive network model of the wall. The numerical solution of the resistive network confirms the usefulness of the simple bounding calculation of the ferromagnetic wall voltage (based on the linear stripline-cylindrical current distribution model). Furthermore, the numerical calculations show agreement in the large and small depth limits with the approximate model. Included in this section is also a treatment of the nonlinear bolt hole voltage for deep penetration compared to the bolt hole radius. The cylindrical ferromagnetic problem is solved for depth of saturation (83) and voltage (84). The corresponding results for linear ramp current are (85) and (86).

11 ACKNOWLEDGEMENTS

The authors would like to thank M. E. Morris, formerly of Sandia National Laboratories, for initiating this study.

12 REFERENCES

[1] M. A. Dinallo and R. J. Fisher, "Voltages Across Assembly Joints Due to Direct-Strike Lightning Currents," Sandia National Laboratories Report, SAND93-0788, August 1994.

[2] K. S. H. Lee (editor), *EMP Interaction: Principles, Techniques, and Reference Data*, Hemisphere Pub. Co., 1986, pp. 454, 455, 464-467.

[3] L. K. Warne and K. C. Chen, "Effective Impedance of Bolt Loads on Narrow Slot Apertures Having Depth," Electromagnetic Waves and Applications, Vol. 6, No. 7, pp. 891-910, 1992.

[4] L. K. Warne and K. O. Merewether, "Approximations to Wire Grid Inductance," Sandia National Laboratories internal memorandum, August 9, 1996.

[5] K. S. Miller and B. Ross, *An Introduction to the Fractional Calculus and Fractional Differential Equations*, John Wiley & Sons, Inc., pp. 44-125.

[6] M. Abramowitz and I. A. Stegun, *Handbook of Mathematical Functions*, Dover Pub., 1972, pp. 299, 1022,1027.

[7] T. C. Chen and A. Papoulis, "Terminal properties of magnetic cores," Proc. IRE, Vol. 46, pp. 839-849, May 1958.

[8] W. A. Johnson and L. K. Warne, "A Steep Front Approximation as the Solution to Nonlinear Diffusion into a Half-Space of Ferromagnetic Material," IEEE Transactions on Magnetics, Vol. 37, no. 5, Sept, 1991, pp. 4322-4327.

Distribution

1	MS0428	T. R. Jones, 12330
2	MS0492	K. C. Chen, 12332
2	MS0405	K. O. Merewether, 12346
2	MS1152	W. A. Johnson, 01652
1	MS1152	R. E. Jorgenson, 01652
1	MS1152	M. Caldwell, 01653
1	MS1152	M. L. Kiefer, 01652
1	MS1152	M. E. Morris, 01652
10	MS1152	L. K. Warne, 01652
2	MS9018	Central Technical Files, 8944
2	MS0899	Technical Library, 04536